Journal of Geoscience and Environment Protection, 2025, 13(11), 45-67
https://www.scirp.org/journal/gep
ISSN Online: 2327-4344
ISSN Print: 2327-4336

Innovative Study on the Occurrence of Iron in the Dam of a Mine in Brazil: Contributions to the Circular Economy

Eduardo da Rosa Aquino[1], Vidal Félix Navarro Torres[1], Romulo Ferraz[2], Carlos Dalmiro[2], Ana Sampaio[2], Carlos Arroyo[3]

[1]Instituto Tecnológico Vale-Mineração, Santa Luzia, Brazil
[2]Vale S.A., Parauapebas, Brazil
[3]Departamento de Engenharia de Minas, Universidade Federal de Ouro Preto, Ouro Preto, Brazil
Email: eduardo.aquino@itv.org, vidal.torres@itv.org, romulo.ferraz@vale.com, carlos.dalmiro@vale.com, ana.sampaio@vale.com, carroyo@ufop.edu.br

How to cite this paper: Aquino, E. R., Navarro Torres, V. F., Ferraz, R., Dalmiro, C., Sampaio, A., & Arroyo, C. (2025). Innovative Study on the Occurrence of Iron in the Dam of a Mine in Brazil: Contributions to the Circular Economy. *Journal of Geoscience and Environment Protection, 13,* 45-67.
https://doi.org/10.4236/gep.2025.1311004

Received: October 8, 2025
Accepted: November 10, 2025
Published: November 13, 2025

Abstract

A geostatistical study was conducted with the objective of developing a better understanding of the sediments deposited in the tailings dam of an iron mine located in Brazil. The samples, derived from two drilling campaigns conducted in 2001 and 2010, were statistically evaluated and validated for the construction of both a 3D geological model and an estimated model. The geological body modeling process was performed using an implicit method, which was based on the interpretation and adjustments of vertical sections and considered the positions of the samples and the grades of the chemical components of interest. In addition, the primitive topography was also considered to determine the base and limits of the deposit, as well as the current topography. The ordinary kriging (OK) method was chosen to estimate the grades of the chemical components and the retained/passing percentages of the particle size fractions described in the samples. The kriging model was validated through two analyses: mean comparison and drift analyses. The total tonnage of the estimated model was 287.14 Mt, with an average Fe grade of 63.89%.

Keywords

Tailings Dam, Geological Model, Ordinary Kriging, Iron Grade

1. Introduction

Tailings dams are engineering works that are used to store materials derived from the ore beneficiation process. Usually, the associated material cannot be recovered

during the physicochemical concentration process and is therefore discarded. Owing to historical mining activity and the lack of specific mineral processing technology for the recovery of fine and ultrafine ores, many tailings dams have highly valuable raw materials that could add value and be commercialized.

In line with the principles of the circular economy, Kefeni et al. (2017) stated that to extend the life cycles of mining processes, evaluating the reuse of tailings is extremely important, as doing so would enable the recovery of precious elements that had previously been planned for disposal. Hunt et al. (2014) noted that it is important to develop, apply and standardize technologies aimed at the circular economy, whose objectives are to integrate mineral production with the treatment and reuse of tailings and thus promote sustainability.

Modeling and estimating tailings bodies are essential for understanding the distributions and natures of the sediments that are present in dams, and these processes play crucial roles in the development of effective mineral extraction strategies. The analysis of these deposits not only guides the process of selecting appropriate methods and mine designs but also contributes to the assessment of possible environmental impacts and the development of sustainable practices.

Geostatistical estimation and simulation methods are valuable tools that can be used to model and estimate or simulate tailings bodies. On the other hand, these methodologies are effective only if they are accompanied by a quality sampling campaign, with well-designed techniques that guarantee greater assertiveness and uncertainty minimization.

According to Vick (1970), the task of modeling tailings bodies is quite complex because great heterogeneity is present in this type of deposit due to sediment deposition. Lottermoser (2010) and Nikonow et al. (2019) also reported that in such a heterogeneous area, zones with low and high grades are derived from exogenous erosive processes, material transport and precipitation. According to Parviainen et al. (2020), this set of characteristics can hinder stationarity, which is a fundamental part of geostatistical modeling methods.

Aquino et al. (2024) emphasized the notion that the application of geostatistical modeling to mine tailings dams is an essential tool for understanding how deposit characteristics vary spatially. This technique uses statistical methods in combination with geographical analysis to examine and represent the heterogeneity of tailings attributes, such as their mineral contents, textures, and grain sizes.

According to Deutsch et al. (2014), the main spatial estimation methods are classified on the basis of their purposes, such as evaluating the spatial distributions of attributes at sites, supporting short-term planning or grade control, and classifying resources and mineral reserves. The methodologies for modeling and estimating tailings deposits are analogous.

In recent decades, some studies have used geostatistical methods to model and estimate tailings bodies. Ordinary kriging (OK) was used in the studies conducted by Louwrens (2016) to estimate the grade of metals such as copper and gold in the Ernest Henry deposit dam; New Century Resources (2017) to estimate the grades of zinc, lead and silver in the dam of a zinc mine; Tripodi et al. (2019)

to estimate the grades of copper, gold and other associated contaminating metals (mercury, arsenic, lead, zinc, nickel and manganese) in two dams in the city of Taltal, Chile; Poseidon Nickel (2020) to estimate the grades of gold, silver, arsenic, copper and nickel in the Windarra dam; and Soto et al. (2022) to estimate the grades of gold, cobalt, copper and iron in the Haveri dam, Finland. The Sequential Gaussian Simulation (SGS) method was used by Blannin et al. (2023) to determine the grades of zinc, lead, copper and indium in the Davidschacht dam, Germany.

In the present study, the geostatistical Ordinary Kriging (OK) method was applied to estimate the grades of iron and other elements present in the tailings of an iron mine dam in Brazil. The main objective was to gain a better understanding of the spatial distribution of Fe across the dam, aiming to identify regions with potentially economically recoverable contents. The following sections present the database, the study methodology, the results obtained, and the conclusions.

2. Database

The database consisted of data derived from two drilling campaigns conducted in 2001 and 2010. In both campaigns, the standard penetration test (SPT) method was used. The obtained samples had records of their grades of the main chemical components linked to the iron ore and of the particle size fractions in certain ranges of interest. There was no record of material density samples; therefore, for the purposes of the developed model, an average density of 2.50 t/m^3 was considered.

In the 2001 campaign, 153 holes were drilled, and 272 samples were recorded. The average distance between the drillholes was 70 m, with a maximum distance of 149 m and a minimum distance of 49 m. The database consisted of 3 types of files: (a) *collar*, with the identity of each hole, the borehole collar coordinates, and the depth of the drillholes; (b) *assay*, with the identity of each hole, the identity of each sample per hole, the initial and final depths of each sample per hole, the total length of the sample, the percentage of the chemical components of each sample as Fe (iron), SiO_2 (silica), P (phosphorus), Al_2O_3 (alumina) and Mn (manganese), and the percentages of particle size fractions at -45 μm and -20 μm; and (c) *survey,* with the identity of each hole, the depth of each hole, and the azimuth and dip of each hole.

In the 2010 campaign, 153 holes were drilled, and 569 samples were recorded. This campaign differed from the 2001 campaign with respect to the characterization of the material, with 529 samples of ore and 40 samples of waste rock. The average distance between the drillholes was 100 m, with a maximum distance of 215 m and a minimum distance of 3 m. The database also comprised 3 types of files: (a) *collar*, with the identity of each hole, the borehole collar coordinates, and the depth of the drillholes; (b) *assay*, with the identity of each hole, the identity of each sample per hole, the initial and final depths of each sample per hole, the total length of the sample, the percentage of the chemical components of each sample

as Fe, SiO_2, P, Al_2O_3, Mn, CaO (calcium oxide), MgO (magnesium oxide), TiO_2 (titanium dioxide) and LOI (loss on ignition), the percentages of the particle size fractions at +250 μm, +150 μm, +106 μm, +75 μm, +45 μm and -45 μm, respectively, and the lithological classifications of ore and waste rock; and (c) *survey,* with the identity of each hole, the depth of each hole, and the azimuth and dip of each hole.

Figure 1 shows the map with the spatial distributions of the samples derived from the 2001 and 2010 campaigns.

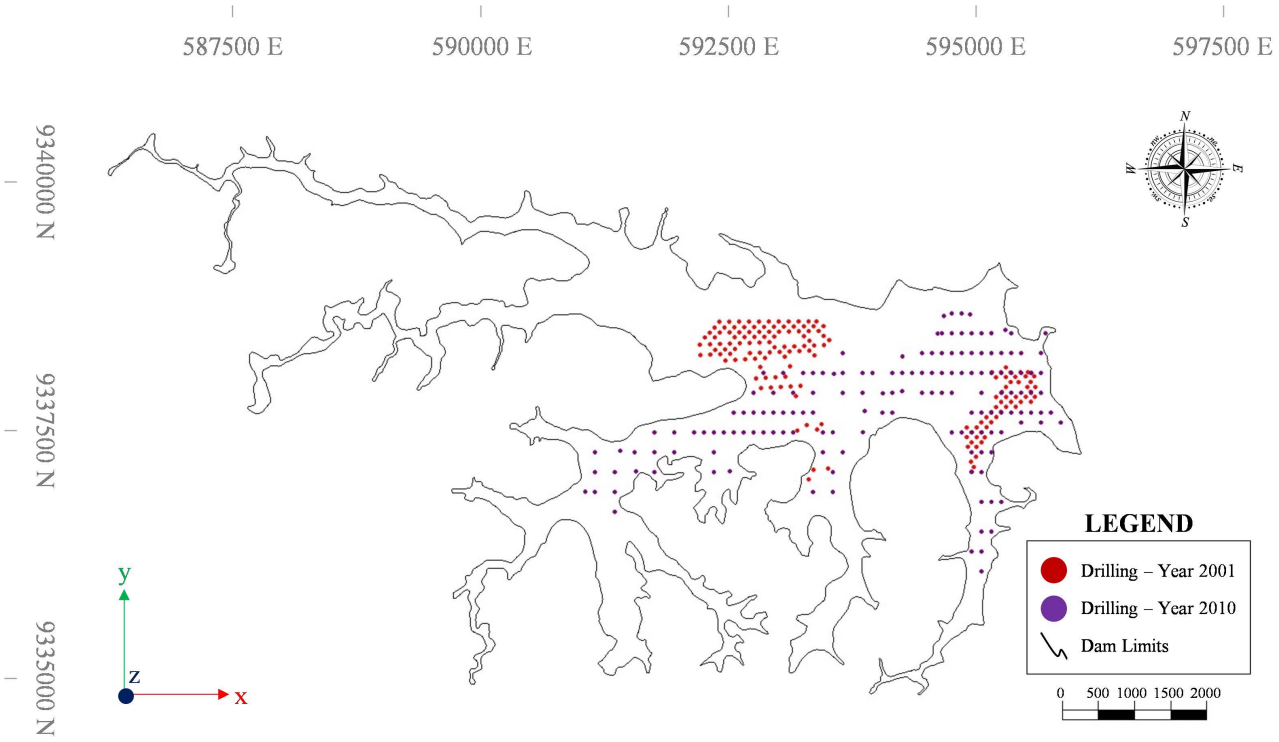

Figure 1. Exploration drilling.

In addition to the drillholes, two topographic surfaces were used: the primitive topography of 1966 and the topography of October 2023. Before its construction, the primitive topography covered the entire area of the dam, in which only the natural vegetation of the terrain was present. The most recent topography comprised the entire dam extension with its delimitation.

3. Materials and Methods

The proposed methodology is aimed at developing a better understanding of the occurrence and deposition of iron tailings sediments in a dam. The method is based on a statistical analysis of samples from drilling campaigns, as well as modeling the tailings body and estimating the model through the ordinary kriging method. A general schematic of the steps employed in the methodology is shown in the flowchart in Figure 2. The steps of the methodology are described in the sections of this chapter.

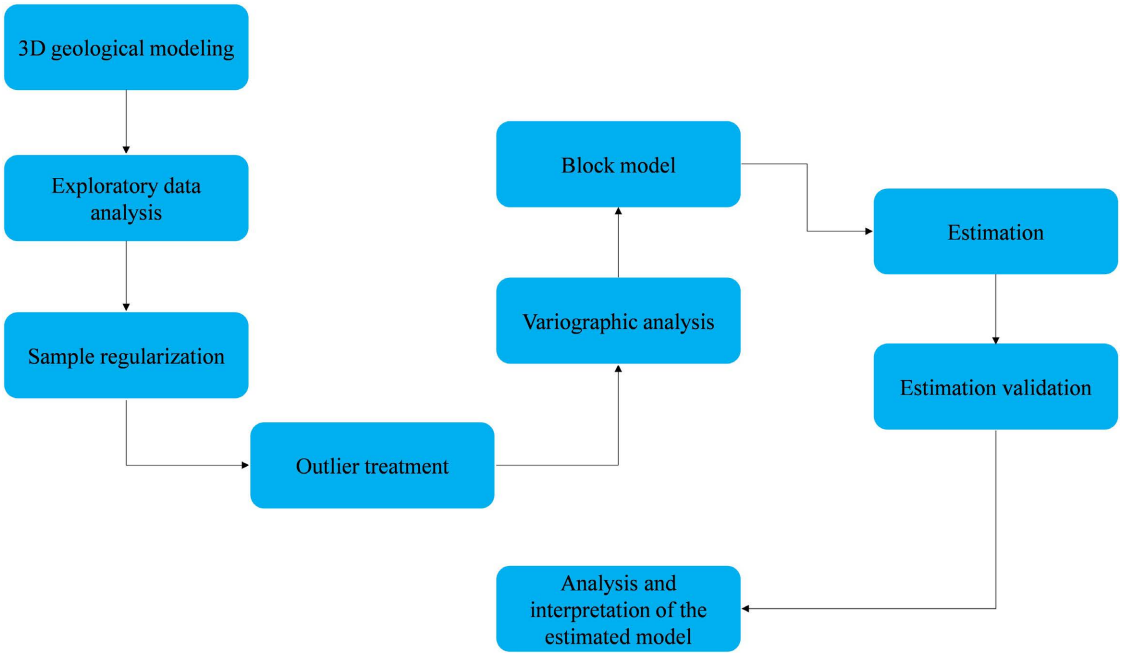

Figure 2. Flowchart of the proposed methodology.

3.1. 3D Geological Modeling

To perform geological modeling on the mineralized tailings body, sections were constructed in the east-west direction, mainly considering the geochemically analyzed sections. In terms of depth, a greater length was prioritized, as the 2010 drilling campaign resulted in greater depths than the 2001 campaign did.

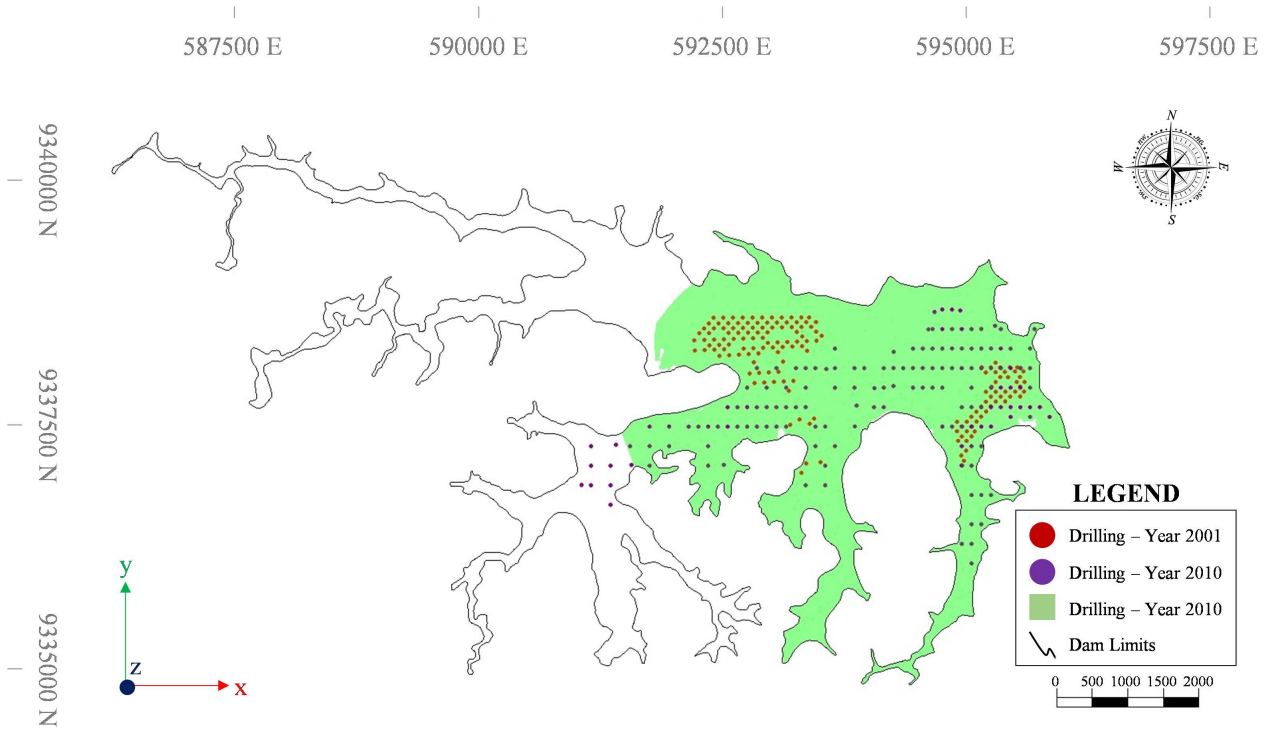

Figure 3. Geological model.

The geological model was developed by combining implicit and explicit techniques. Implicit techniques were applied in the automatic interpolation of grades between drill holes, allowing the continuous construction of the volumetric model and the generation of grade estimates in areas with lower sampling density. Explicit techniques, on the other hand, involved the manual interpretation of sections, including local adjustments to the geometry of the tailings body and the interfaces between zones of different grades, ensuring that geological features observed in the original data were accurately preserved. A plan view of the model, including its drillholes, is shown in Figure 3. The topography of 2023 was used to vertically delimit the model. The primitive topography was used to delimit the model laterally so that its edges would be smoother and not vertical. The total volume of the model was 118.85 Mm^3, and, assuming a density of 2.50 t/m^3, the resulting tonnage was 297.13 Mt.

3.2. Exploratory Data Analysis

In geostatistics, basic statistical tools, such as histograms and boxplots, are commonly used to better understand a sample population. Such tools allow for a better understanding of the behaviors of the samples through what is referred to as exploratory data analysis. Comparisons among the means, variances, upper quartiles, histogram formats, etc., of different groups help with making future decisions and in terms of the knowledge of the variables under study by summarizing them in the forms of graphical and statistical interpretations.

Owing to the chronological tailings deposition distance between the two campaigns and to verify whether there were significant differences between the basic statistics of different drilling campaigns, the analyses were performed in different ways. First, each drilling campaign was analyzed separately. Afterward, an analysis was performed by combining the databases of the two campaigns. For all statistics, sample length-based weighting was applied.

Table 1 presents a statistical summary of the samples acquired from the drilling campaign in 2001, and Table 2 presents a statistical summary of the year 2010. Table 3 presents a summary of the analysis conducted on both campaigns together. Figure 4 shows the histogram and boxplot of Fe grades considering the combination of the two campaigns.

Table 1. Statistical summary of the samples derived from the 2001 drilling campaign.

Variable	Mean (%)	Variance (%²)	Standard deviation (%)	Coefficient of variation (%)	Number of samples	Min. (%)	P_5 (%)	P_{50} (%)	P_{95} (%)	Max. (%)
Fe	65.01	0.71	0.84	0.01	272	59.56	63.83	65.04	66.25	66.77
SiO_2	1.12	0.23	0.48	0.43	272	0.58	0.72	1.03	1.64	5.76
P	0.07	0.00	0.01	0.18	272	0.04	0.05	0.07	0.09	0.12
Al_2O_3	1.91	0.17	0.42	0.22	272	1.02	1.30	1.87	2.52	4.41
Mn	0.85	0.08	0.29	0.34	272	0.32	0.45	0.81	1.34	2.06
−45 μm	70.77	214.16	14.63	0.21	272	0.00	44.91	72.25	89.14	96.80
−20 μm	56.62	248.39	15.76	0.28	272	0.00	24.45	57.80	80.23	96.59

Table 2. Statistical summary of the samples derived from the 2010 drilling campaign.

Variable	Mean (%)	Variance (%²)	Standard deviation (%)	Coefficient of variation (%)	Number of samples	Min. (%)	P_5 (%)	P_{50} (%)	P_{95} (%)	Max. (%)
Fe	63.14	2.02	1.42	0.02	529	56.56	60.88	63.11	65.52	66.46
SiO_2	2.84	0.72	0.85	0.30	529	0.92	1.70	2.77	4.04	10.40
P	0.05	0.00	0.01	0.21	529	0.03	0.03	0.05	0.06	0.11
Al_2O_3	2.61	0.48	0.69	0.27	529	0.75	1.45	2.64	3.76	4.56
Mn	0.77	0.04	0.20	0.26	529	0.39	0.48	0.80	1.13	1.44
CaO	0.02	0.00	0.01	0.48	529	0.01	0.01	0.02	0.02	0.30
MgO	0.06	0.00	0.02	0.33	529	0.02	0.04	0.06	0.08	0.72
TiO_2	0.17	0.00	0.04	0.26	529	0.04	0.10	0.18	0.24	0.30
LOI	2.92	0.27	0.52	0.18	529	1.23	1.96	2.96	3.70	4.58
+250 μm	1.45	9.40	3.07	2.11	529	0.00	0.00	0.40	6.31	27.40
+150 μm	1.53	4.53	2.13	1.39	529	0.00	0.00	0.70	5.79	15.20
+106 μm	2.52	8.89	2.98	1.19	529	0.00	0.00	1.50	8.99	18.80
+75 μm	5.86	34.99	5.91	1.01	529	0.00	0.10	3.60	17.03	25.80
+45 μm	9.07	72.01	8.49	0.94	529	0.00	0.30	6.10	25.98	36.20
−45 μm	79.57	327.66	18.10	0.23	529	26.00	45.38	85.54	99.20	100.00

Table 3. Statistical summary of the samples derived from the 2001 and 2010 drilling campaigns.

Variable	Mean (%)	Variance (%²)	Standard deviation (%)	Coefficient of variation (%)	Number of samples	Min. (%)	P_5 (%)	P_{50} (%)	P_{95} (%)	Max. (%)
Fe	64.09	2.23	1.49	0.02	801	56.56	61.41	64.46	66.10	66.77
SiO_2	1.97	1.21	1.10	0.56	801	0.58	0.81	1.69	3.84	10.40
P	0.06	0.00	0.01	0.26	801	0.03	0.04	0.06	0.08	0.12
Al_2O_3	2.26	0.45	0.67	0.30	801	0.75	1.36	2.09	3.47	4.56
Mn	0.81	0.06	0.25	0.31	801	0.32	0.47	0.80	1.28	2.06
CaO	0.02	0.00	0.01	0.48	529	0.01	0.01	0.02	0.02	0.30
MgO	0.06	0.00	0.02	0.33	529	0.02	0.04	0.06	0.08	0.72
TiO_2	0.17	0.00	0.04	0.26	529	0.04	0.10	0.18	0.24	0.30
LOI	2.92	0.27	0.52	0.18	529	1.23	1.96	2.96	3.70	4.58
+250 μm	1.45	9.40	3.07	2.11	529	0.00	0.00	0.40	6.31	27.40
+150 μm	1.53	4.53	2.13	1.39	529	0.00	0.00	0.70	5.79	15.20
+106 μm	2.52	8.89	2.98	1.19	529	0.00	0.00	1.50	8.99	18.80
+75 μm	5.86	34.99	5.91	1.01	529	0.00	0.10	3.60	17.03	25.80
+45 μm	9.07	72.01	8.49	0.94	529	0.00	0.30	6.10	25.98	36.20
−45 μm	79.57	327.66	18.10	0.23	529	26.00	45.38	85.54	99.20	100.00
−20 μm	56.62	248.39	15.76	0.28	272	0.00	24.45	57.80	80.23	96.59

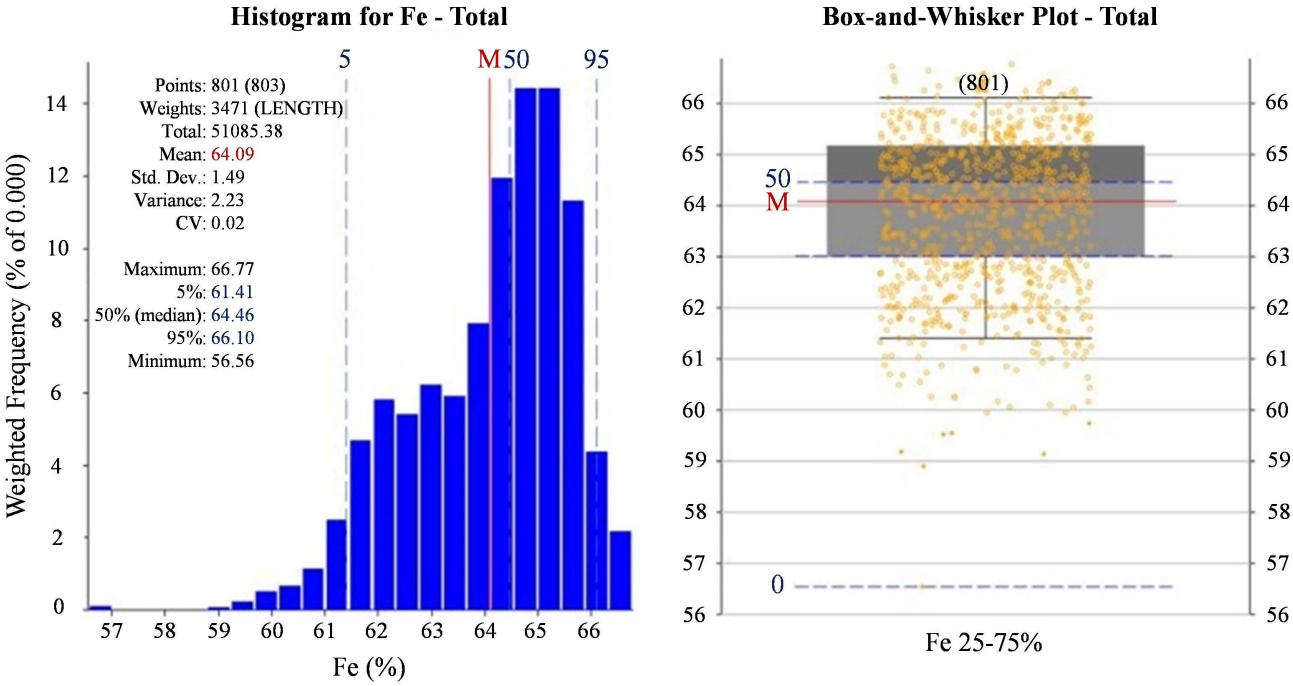

Figure 4. Fe grade histogram and boxplot for the combination of the two campaigns years of 2001 and 2010.

The tables show that the samples had low variability in each element. Furthermore, it is noteworthy that the grades of Fe were homogeneous, with less than 5% of the samples having Fe grades lower than 60%. This finding demonstrates that the tailings stored in the dam have grades with the possibility of economic viability.

3.3. Sample Regularization

Sample regularization was performed to ensure that the samples had the same support within a mineralized domain, where the data were in a format that was suitable for modeling and estimation tasks. This approach helped to reduce the variability and heterogeneity of the data, allowing the spatial parameters to be better estimated. In addition, adopting this approach ensured that the samples were evenly distributed in space. For the samples derived from the drilling campaigns of 2001 and 2010, a sample support analysis was performed, as shown in **Figure 5**.

The samples from 2001 had a mean length of 6.43 m, and 50% of the samples had lengths less than 6.50 m (median). The maximum value was 10.30 m, and 90% of the data had lengths between 4.11 m and 8.22 m. Now, considering the samples from 2010, the average length was 3.25 m, with a median of 4.50 m. The maximum value was 15 m, and 90% of the data had lengths between 1 m and 5 m. When grouping the samples acquired from the two drilling campaigns, it was observed that the median was 5 m. Therefore, this was the length that was defined for the regularization of the samples, with minimum composites of 2.50 m. The leveling was defined as a redistribution implemented along all the composites of the residual at the end of the hole below the minimum of 2.50 m. Thus, the average length and the median of the regularized samples were both 5 m. **Table 4** presents a sta-

tistical summary of the samples derived from the drilling campaigns in 2001 and 2010 after applying the sampling support change.

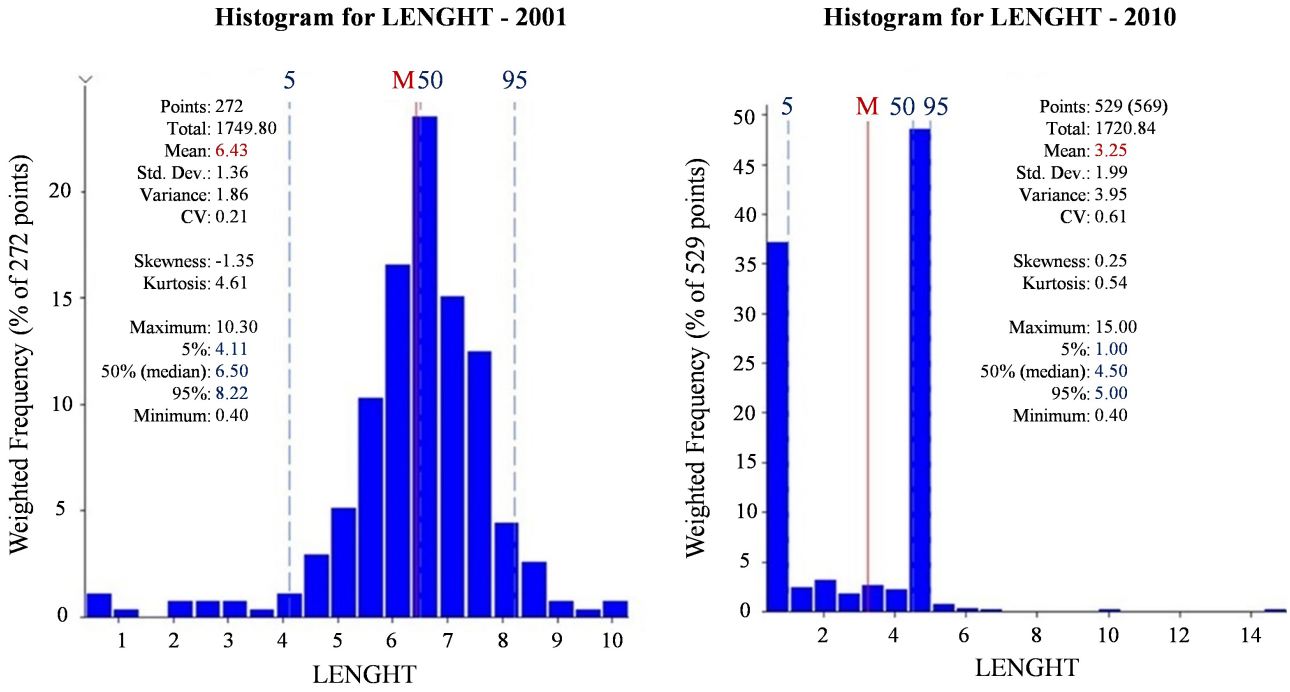

Figure 5. Sample support histograms for the samples derived from 2001 and 2010.

Table 4. Statistical summary of the samples derived from the 2001 and 2010 drilling campaigns after applying the sampling support change.

Variable	Mean (%)	Variance (%²)	Standard deviation (%)	Coefficient of variation (%)	Number of samples	Min. (%)	P_5 (%)	P_{50} (%)	P_{95} (%)	Max. (%)
Fe	64.09	2.12	1.46	0.02	686	57.64	61.45	64.44	66.07	66.77
SiO_2	1.97	1.17	1.08	0.55	686	0.58	0.81	1.72	3.82	9.22
P	0.06	0.00	0.01	0.25	686	0.03	0.04	0.06	0.08	0.12
Al_2O_3	2.26	0.42	0.65	0.29	686	0.75	1.42	2.10	3.43	4.41
Mn	0.81	0.06	0.25	0.31	686	0.32	0.47	0.80	1.27	2.06
CaO	0.02	0.00	0.01	0.32	343	0.01	0.01	0.02	0.02	0.08
MgO	0.06	0.00	0.01	0.24	343	0.03	0.04	0.06	0.08	0.22
TiO_2	0.17	0.00	0.04	0.25	343	0.04	0.10	0.18	0.24	0.30
LOI	2.92	0.25	0.50	0.17	343	1.63	1.99	2.98	3.63	4.14
+250 μm	1.45	8.03	2.83	1.96	343	0.00	0.00	0.48	6.16	24.82
+150 μm	1.53	3.80	1.95	1.28	343	0.00	0.00	0.80	5.60	11.27
+106 μm	2.52	7.69	2.77	1.10	343	0.00	0.00	1.66	8.27	13.80
+75 μm	5.87	31.22	5.59	0.95	343	0.00	0.19	3.88	16.71	25.80
+45 μm	9.08	65.38	8.09	0.89	343	0.00	0.42	6.14	24.65	35.30
−45 μm	75.10	265.72	16.30	0.22	686	8.81	45.79	76.87	97.50	99.99
−20 μm	56.56	231.70	15.22	0.27	343	5.47	24.48	57.85	79.33	96.59

3.4. Outlier Treatment

To determine outliers, the analytes and particle size fractions of the samples were evaluated in terms of their basic statistics using various tools, such as frequency histograms, box plots, log probability plots, mean and variance plots and cumulative plots. These graphs, when used together, provided a complete view of the data distribution, facilitating the visualization of anomalous values or outliers.

When the data were analyzed, the SiO_2, P, MgO and -45 μm variables exhibited anomalous values. Thus, the top-cut or bottom-cut technique was used to limit the influence of outliers during the modeling and estimation processes and to avoid distortions. That is, the top-cut and bottom-cut methods limited the maximum and minimum values of the outliers, respectively, to predefined maximum and minimum values. Therefore, the following values were defined for the aforementioned variables: (a) top-cut – SiO_2 = 5.09%, P = 0.10% and MgO = 0.10%; (b) bottom-cut – -45 μm = 24.75%.

Table 5 presents a statistical summary of the variables produced after the application of the cuts. This application did not significantly affect the means of the variables, with differences of less than 1% relative to the original data.

Table 5. Statistical summary of the samples derived from the drilling campaigns of 2001 and 2010 after the cuts were applied.

Variable	Mean (%)	Variance (%²)	Standard deviation (%)	Coefficient of variation (%)	Number of samples	Min. (%)	P_5 (%)	P_{50} (%)	P_{95} (%)	Max. (%)
SiO_2	1.96	1.11	1.05	0.54	686	0.58	0.81	1.72	3.82	5.09
P	0.06	0.00	0.25	0.25	686	0.03	0.04	0.06	0.08	0.10
MgO	0.06	0.00	0.01	0.20	343	0.03	0.04	0.06	0.08	0.10
−45 μm	75.58	240.95	15.52	0.21	686	24.99	47.89	76.97	97.50	99.99

3.5. Variographic Analysis

Variography is the main tool that is used in geoscience to measure spatial continuity. Through a variogram, it is possible to determine a mathematical equation that effectively describes the behavior of the geological phenomenon of interest, showing the directions in which and the distances at which there is a greater correlation between the samples.

A variogram is a model that represents spatial variability and is a very important tool in geostatistics because it supports interpolation techniques (for example, kriging). It measures the degree of similarity between a value acquired from an unsampled location and a sample near this location.

According to Journel and Huijbregts (1978), the variogram function, named $2\gamma(h)$, is the mathematical expectation of the square of the difference between pairs of points separated by a distance (h). Equation 1 demonstrates what was stated above.

$$2\gamma(h) = E\left\{\left[z(u) - z(u+h)\right]^2\right\} \quad \text{(Equation 1)}$$

As mathematical expectation can be represented by a summation, the variogram function can be rewritten in another way to facilitate its understanding and the calculation of values (Davis, 2002). Equation 2 shows how this calculation was performed. As the equation isolated the unknown, i.e., by calculating half of the variogram, it became known as a semivariogram.

$$\gamma(h)=\frac{1}{2\cdot n}\sum_{i=1}^{n}\left[z(u)-z(u+h)\right]^2 \qquad \text{(Equation 2)}$$

where "$\gamma(h)$" is the semivariogram, "n" is the number of pairs of samples, "$z(u)$" are the samples that are spatially located in a given location and "$z(u+h)$" are the samples that are located at a distance h from $z(u)$. The distance h is a vector, with a magnitude and a direction. In the literature, many authors end up referring to semivariograms simply "variograms"; this convention will be followed hereafter.

The variogram was represented by means of a graph. Each point of this graph was generated via Equation 2 for all values of h. It was expected that with increasing distance, the variability of the phenomenon would increase. However, there was a point where increasing the distance did not imply an increase in the squared difference between the pairs.

A variogram has several important elements, which are as follows.

a) Sill: the plateau reached by the variogram as the distance h increases. Its value approximates the total variance of the sample values (prior variance of the data).

b) Range: distance at which the variogram reaches the plateau.

c) Nugget Effect: the vertical jump from the 0 value at the origin to the variogram values at extremely small separation distances. However, for $\gamma(0) = 0$, the sampling errors added to the measurement errors ultimately generate this discontinuity at the origin of the variogram.

Independent variographic analyses were performed for all analytes of the samples derived from the drilling campaigns of 2001 and 2010 together. For the particle size fractions, the average variogram of the -45 μm fraction (the most representative fraction) was used.

All the variograms were modeled after applying the top-cut/bottom-cut method, which enabled the generation of more robust and adequate variograms. In addition, each of the variograms had two spherical structures, each with its sill contribution (C_1 and C_2) and ranges (a_1, a_2 and a_3) in the three continuity directions (x, y, and z). Table 6 presents a summary of the parameters used to model the variograms. The modeled Fe variograms are shown in Figure 6.

Table 6. Summary of the parameters used to model the variograms.

		First spherical structure				Second spherical structure			
Variable	Rotation angle in Z (grid)	C_1(%²)	a_1(m)	a_2(m)	a_3(m)	C_2(%²)	a_1(m)	a_2(m)	a_3(m)
Fe	−10	0.24	311	435	60	0.64	1223	694	80
SiO_2	−10	0.17	96	220	58	0.82	1088	541	80
P	−10	0.64	215	229	45	0.35	1039	748	80

Continued

Al_2O_3	−10	0.26	129	272	39	0.62	1200	783	60
Mn	0	0.57	195	163	35	0.42	633	784	165
CaO	0	0.38	81	116	6	0.60	1100	255	45
MgO	10	0.20	184	128	29	0.65	914	483	100
TiO_2	30	0.24	305	232	5	0.60	1023	578	98
LOI	−20	0.30	288	174	14	0.59	834	868	50
−45 μm	−20	0.47	100	310	31	0.48	690	406	34

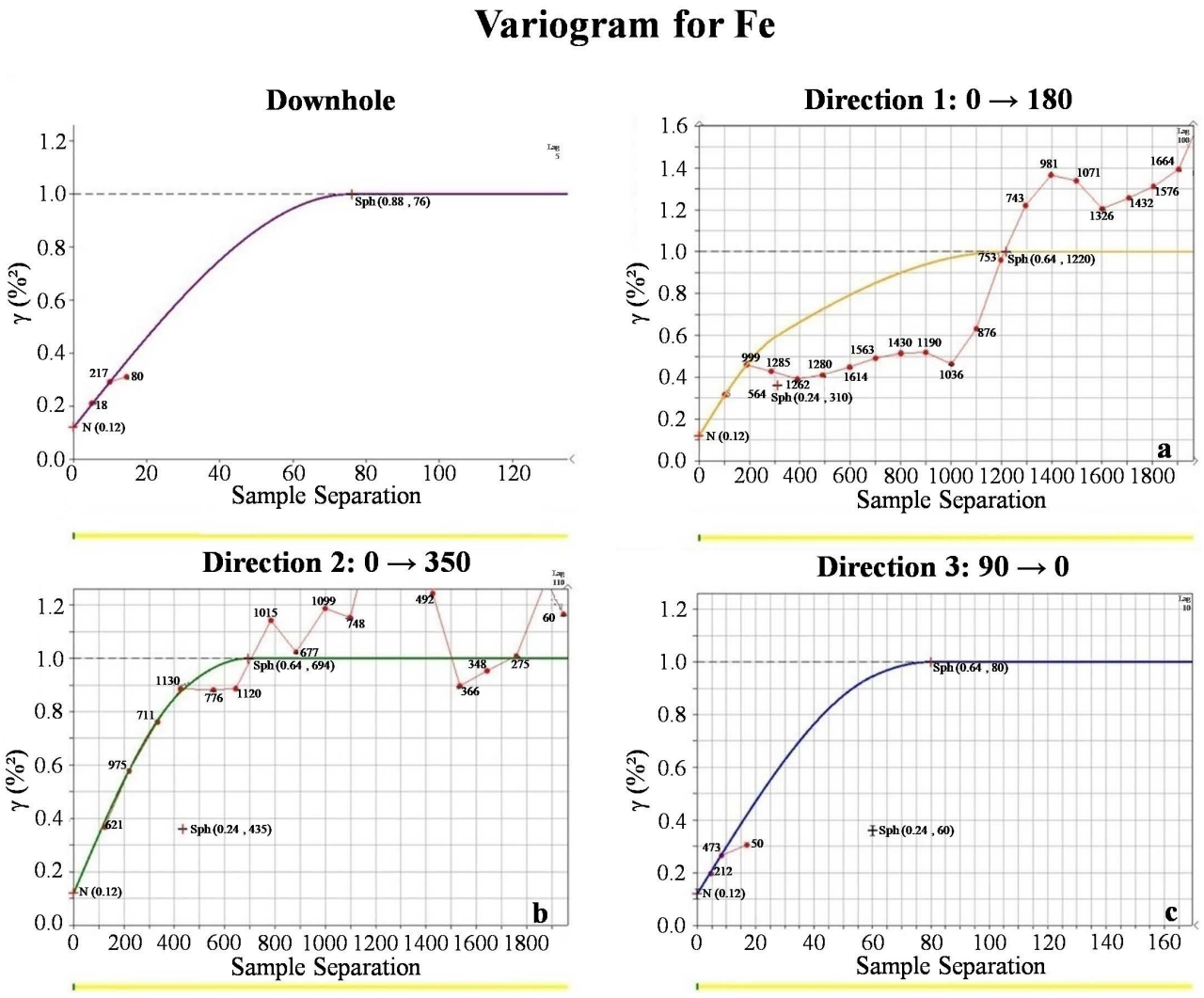

Figure 6. Variograms modeled for variable Fe: (a) direction 1; (b) direction 2; (c) direction 3.

3.6. Block Model

To perform the estimation process, a block model was created in a predefined grid, which included the entire dam region and not only the region of the drilling campaigns. The information derived from the grid and the block model are presented in Table 7. Notably, the model was not rotated.

Table 7. Grid and block model information.

	X (East-West)	Y (North-South)	Z (Elevation)
Origin coordinates of the grid (m)	586,240	9,334,830	180
Number of blocks in each direction	394	228	18
Size of the blocks (m)	25	25	5
Size of the subblocks (m)	3.125	3.125	0.5

The resulting block model had a volume of 117.84 Mm^3. Compared with the volume of the geological model of (118.85 Mm^3), there is a difference of 0.85%. Therefore, it can be said that there was good adherence between the models, as it was within the acceptable limit of 2%.

3.7. Estimation

Several estimation techniques are available for predicting values in unsampled areas. Among the classic interpolators, the principle is generally the same: assign weights to the given samples using weighted averaging algorithms. However, these methods do not consider sample support or patterns of spatial variability. Furthermore, they do not provide a measure of the induced estimation error. In this sense, it is necessary to use an interpolator known as kriging.

Kriging was developed by Georges Matheron in France in the 1960s and is named after the mining engineer Daniel G. Krige, who pioneered the use of moving averages to avoid systematically overestimating mining reserves (Delfiner & Delhomme, 1975).

The difference between kriging and other interpolation methods is the way in which the weights are assigned to the different samples. The procedure for interpolating values in kriging is similar to that of interpolation via a weighted moving average; however, the weights assigned to each sample are related to the distance of each sample from the estimated point, as well as to the spatial dependence between the samples given by the corresponding variogram.

Furthermore, this method provides an unbiased estimate with a minimum error variance. That is, the difference between the estimated and true values for the same point is zero, and the error variance is the smallest ang those of all the other estimators. In view of these characteristics, kriging is known as a best linear unbiased estimate (BLUE) interpolator (Isaaks & Srivastava, 1989): linear because the data estimated by ordinary kriging correspond to weighted linear combinations of the available data, unbiased because the mathematical expectation of the error is zero, and best because it aims to minimize the variance of the estimate (kriging variance).

Kriging encompasses a set of estimation methods, among which OK was chosen in this study to perform the estimation process. The OK approach can be represented by Equation 3, where "$z^*(u)$" is the estimated value, "$z(u_i)$" is the value of each sample, "$m(u)$" is the local mean and "$\lambda_i(u)$" is the weight assigned to each sample.

$$z^*(u) - m(u) = \sum_{i=1}^{n} \lambda_i(u) \cdot \left[z(u_i) - m(u_i) \right] \quad \text{(Equation 3)}$$

The OK principle does not presuppose knowledge of the local mean or the stationarity of the mean in the sample field. In addition, the estimate needs to be unbiased; thus, the sum of all the weights is assumed to be equal to one, as shown in Equation 4.

$$\sum_{i=1}^{n} \lambda_i(u) = 1 \quad \text{(Equation 4)}$$

When the nonbiased condition was satisfied, the system of equations gained one more equation; however, the number of unknowns (weights) remained the same. For the system to have the same numbers of equations and unknowns, an "artificial" variable was created, i.e., a Lagrangian multiplier. Thus, the function that minimized the error variance is given by Equation 5, which is presented in matrix form in Equation 6.

$$\sum_{j=1}^{n} \lambda_j \cdot C(u_i, u_j) - \mu = C(u, u_i) \quad \text{(Equation 5)}$$

$$\begin{bmatrix} C_{11} & C_{12} & C_{13} & C_{14} & \cdots & C_{1n} \\ C_{21} & \ddots & C_{23} & C_{24} & \cdots & C_{2n} \\ C_{31} & C_{32} & \ddots & C_{34} & \cdots & C_{3n} \\ C_{41} & C_{42} & C_{43} & \ddots & \cdots & C_{4n} \\ \vdots & \vdots & \vdots & \vdots & \ddots & \vdots \\ C_{n1} & C_{n2} & C_{n3} & C_{n4} & \cdots & C_{nn} \\ 1 & 1 & 1 & 1 & 1 & 0 \end{bmatrix} \cdot \begin{bmatrix} \lambda_1 \\ \lambda_2 \\ \lambda_3 \\ \lambda_4 \\ \vdots \\ \lambda_n \\ \mu \end{bmatrix} = \begin{bmatrix} C_{u1} \\ C_{u2} \\ C_{u3} \\ C_{u4} \\ \vdots \\ C_{un} \\ 1 \end{bmatrix}. \quad \text{(Equation 6)}$$

where "λ_j" denotes the weights of the samples, "$C(u_i, u_j)$" is the covariance between samples, "μ" is the Lagrangian multiplier and "$C(u, u_j)$" is the covariance between the samples and the location to be estimated.

4. Results and Discussions

4.1. Estimation Strategy Using Ordinary Kriging

The OK estimation strategy was performed using the cross-validation technique, where variations in the search radii of the ellipsoid, the minimum and maximum quantities of samples used in the estimation process and the maximum number of samples used per hole were tested. The search radii of the ellipsoid were chosen as a function of the variance of the Fe variograms.

The radius of the maximum, average and minimum distances of the search ellipsoid were varied to 70%, 80% and 100% of the prior variance of the variogram, respectively. Thus, the respective radii were 460 x 300 x 35, 600 x 360 x 43 and 1,223 x 694 x 80. In addition, minimum amounts of 3, 4, 5 and 6 samples and maximum amounts of 12, 18, 24, 30 and 32 samples were observed. Two situations

were also tested, one without a defined maximum number of samples per hole and another with a defined maximum of 3 samples per hole.

After the numerous possibilities were tested and all the mentioned parameters were varied, the estimation parameters were defined as follows: a search ellipsoid with a radius of 600 × 360 × 43, a minimum of 5 samples, a maximum of 32 samples and maximum of 3 samples per hole. Two other searches were also performed, with factors of 100% and 200% in relation to the defined estimate. Thus, the blocks for which no estimates were obtained in any of the three trials did not satisfy the minimum continuity criteria and were not estimated. A plan view of the estimated model for Fe, which corresponded to a tonnage of 287.14 Mt with an average Fe grade of 63.89%, is shown in Figure 7.

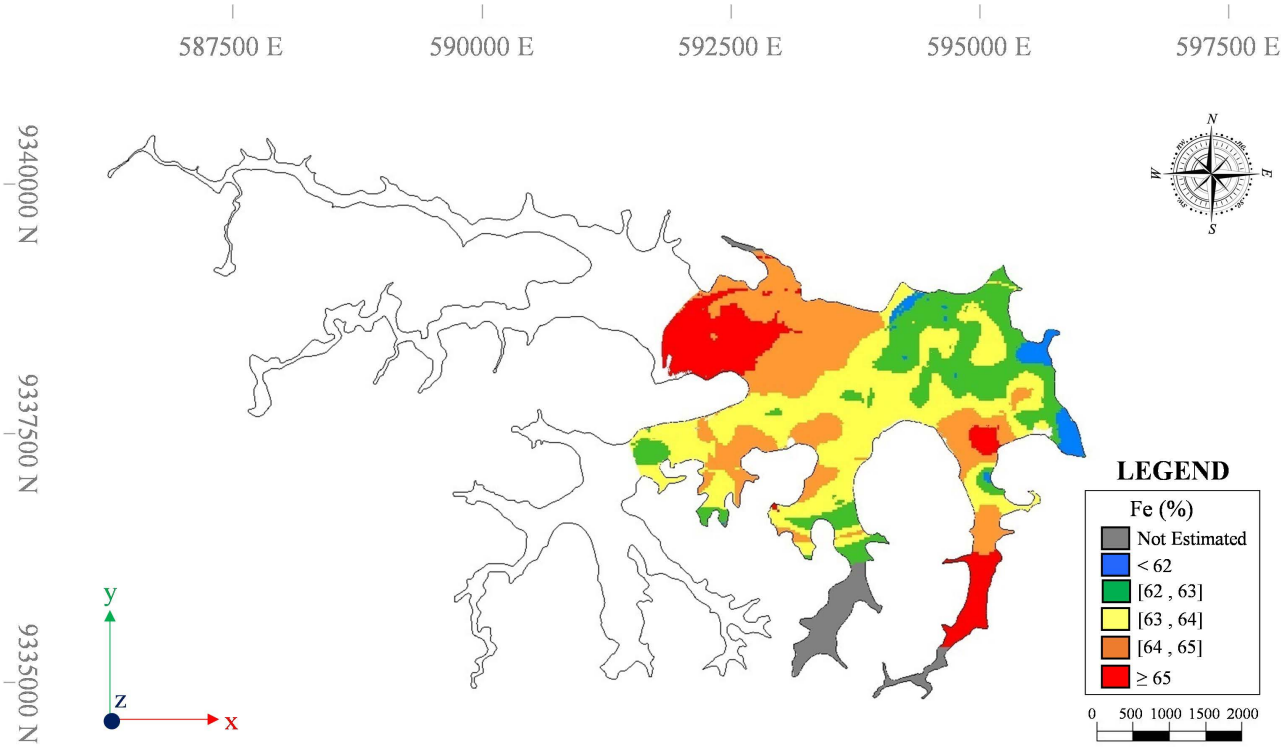

Figure 7. Plan view of the estimated block model for Fe.

4.2. Estimation Validation

The estimate was validated through an independent verification, with the purpose of evaluating the performance and compliance of the kriging method on the basis of the original data. Thus, two validations were used to verify the results: (i) a comparison between global means and (ii) a drift analysis.

4.2.1. Comparison between Global Averages

When global averages are compared, the average of the model estimated by kriging is expected to be somewhat similar to the average of the model estimated by the nearest-neighbor (NN) method. A variation of 10% between the means is considered acceptable, although it is advisable to verify the parameters of the es-

timate to improve the obtained results.

For the estimates of the iron element, the model mean estimated by OK was 63.89%, against an average of 63.84% of the estimate yielded by the NN method. The difference between the estimates was approximately 0.1%, with the OK estimate slightly overestimated in relation to that of the NN method. This difference was insignificant and was within the acceptable range. The histograms of the OK and NN estimates of Fe are shown in Figure 8.

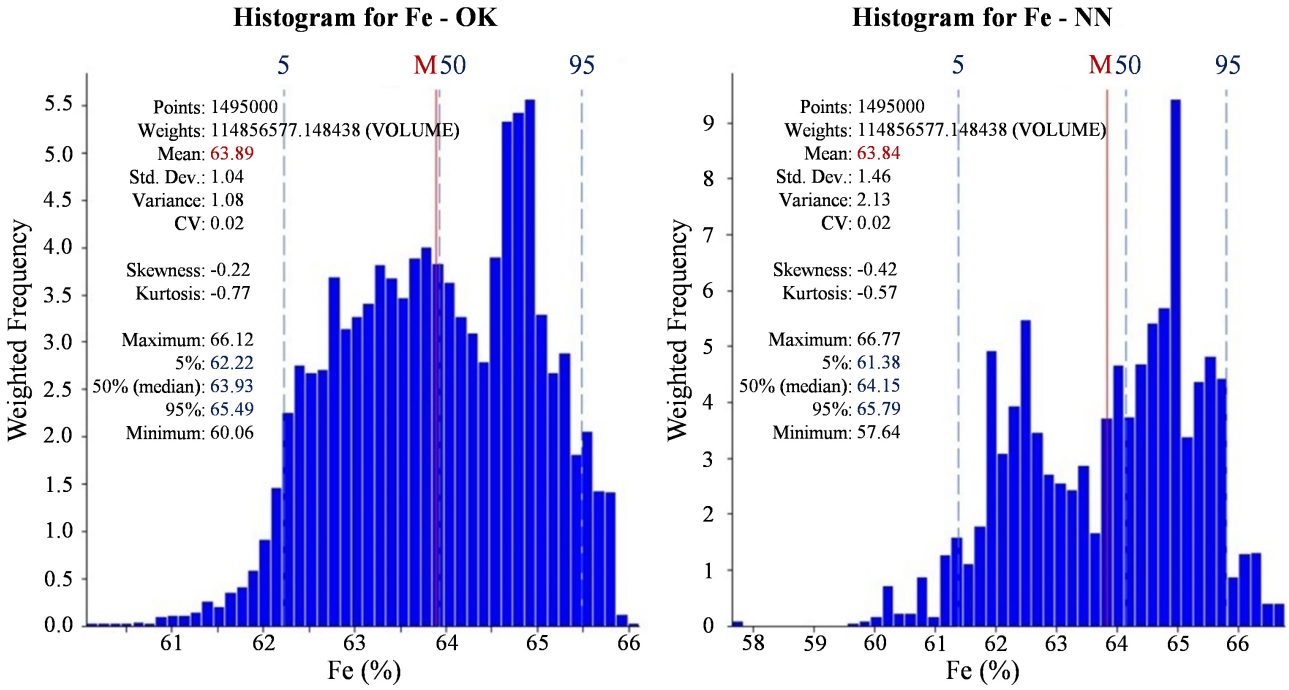

Figure 8. Histograms of the means of the OK and NN estimates produced for the Fe grade.

4.2.2. Drift Analysis

A drift analysis, also known as a swath plot, is aimed at evaluating the local bias of an estimation method, verifying whether the estimated values, on average, follow the trend of the underlying data. This type of analysis consists of performing a comparison between the averages of the OK estimate and the average of the samples, or even the average of another estimate (for example, NN). This tool makes it possible to visualize and compare the spatial distributions of the input data and the estimate along predefined ranges or slices in the estimated model. Thus, local deviations, biases and imprecision can be identified.

In general, the band along the data to be analyzed is defined as a function of the direction of the drilling grid. The strips can have different dimensions but generally have widths of 4 to 6 times the width of the blocks. After this definition step, the averages of the samples and the averages of the estimates obtained in each range are calculated. Thus, graphical analyses of these averages, as well as the number of samples used in each band and the impacted masses per band, are performed to understand the reliability of the analyzed data.

A good fit between the graphs of the estimate and the samples means a lower

local bias and suggests that the estimate produced by kriging is acceptable. In general, the comparative analysis between the kriged model and the samples in the regions with the greatest numbers of samples and more representative masses revealed good adherence, as shown in Figure 9, considering the element Fe.

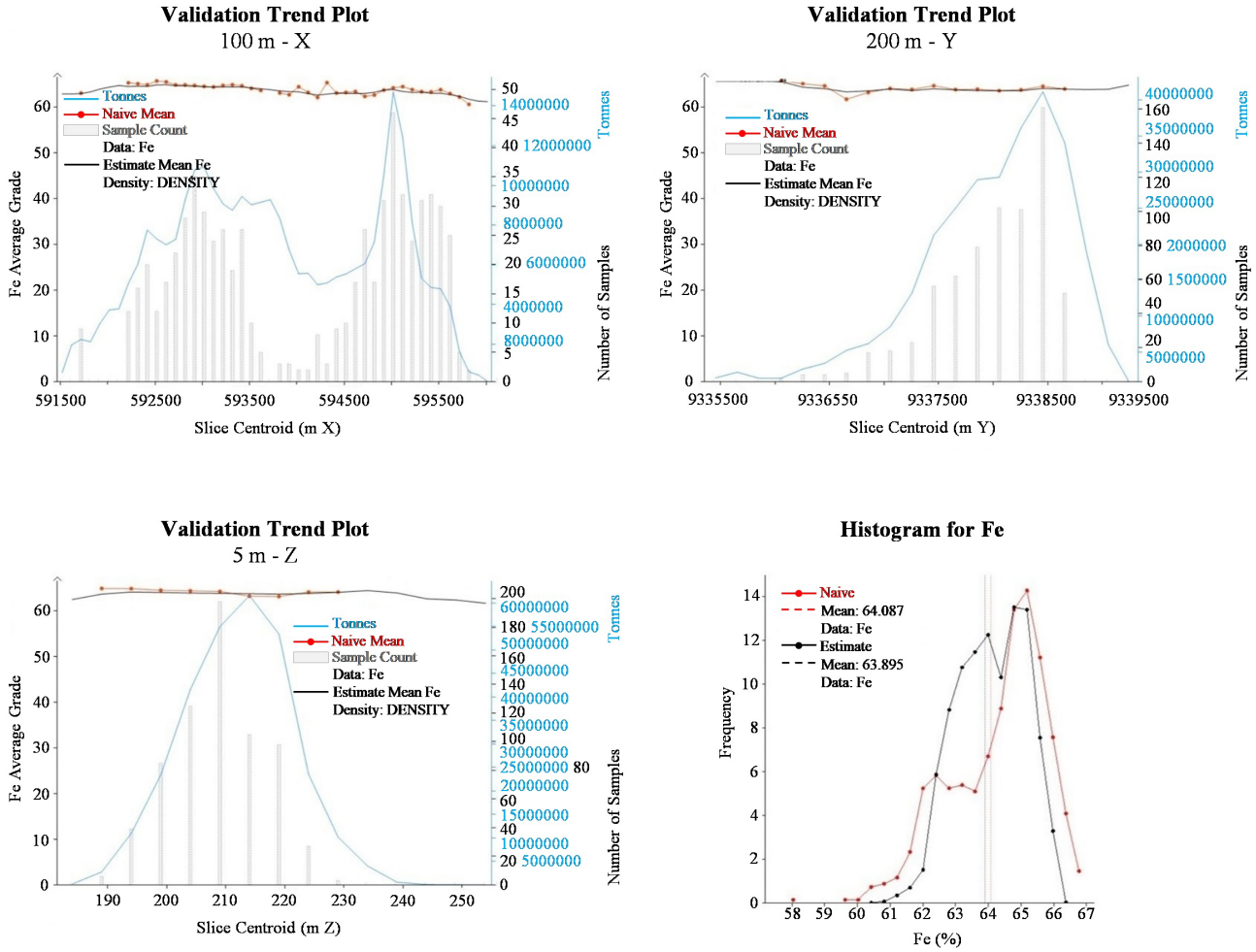

Figure 9. Drift analysis of Fe along the X, Y, and Z directions based on swath plots.

4.3. Analysis and Interpretation of the Estimated Model

The estimated model had an average Fe grade of 63.89%, with a standard deviation of 1.04%. The minimum Fe grade was 60.06%, and the maximum grade was 66.12%. In addition, 80% of the blocks in the model had Fe grades between 62.22% and 65.49%, with a median of 63.93%.

To evaluate the behavior of Fe at various depths, some sections of the block model were constructed at different depths. The sections at 234.50 m, 229.50 m, 219.50 m and 214.50 m are shown in Figures 10-13, respectively.

The regions at the southern end of the dam were the ones with the highest model elevations (234.50 m and 229.50 m) and coincided in regions with high grades, reaching Fe values greater than 65%. However, these zones are sparsely sampled, which increases the likelihood of an overestimation bias. This limitation

highlights the need to carry out additional drilling campaigns in these areas to obtain more representative data and reduce the uncertainty associated with the geostatistical model. The inclusion of new boreholes will allow for a more refined

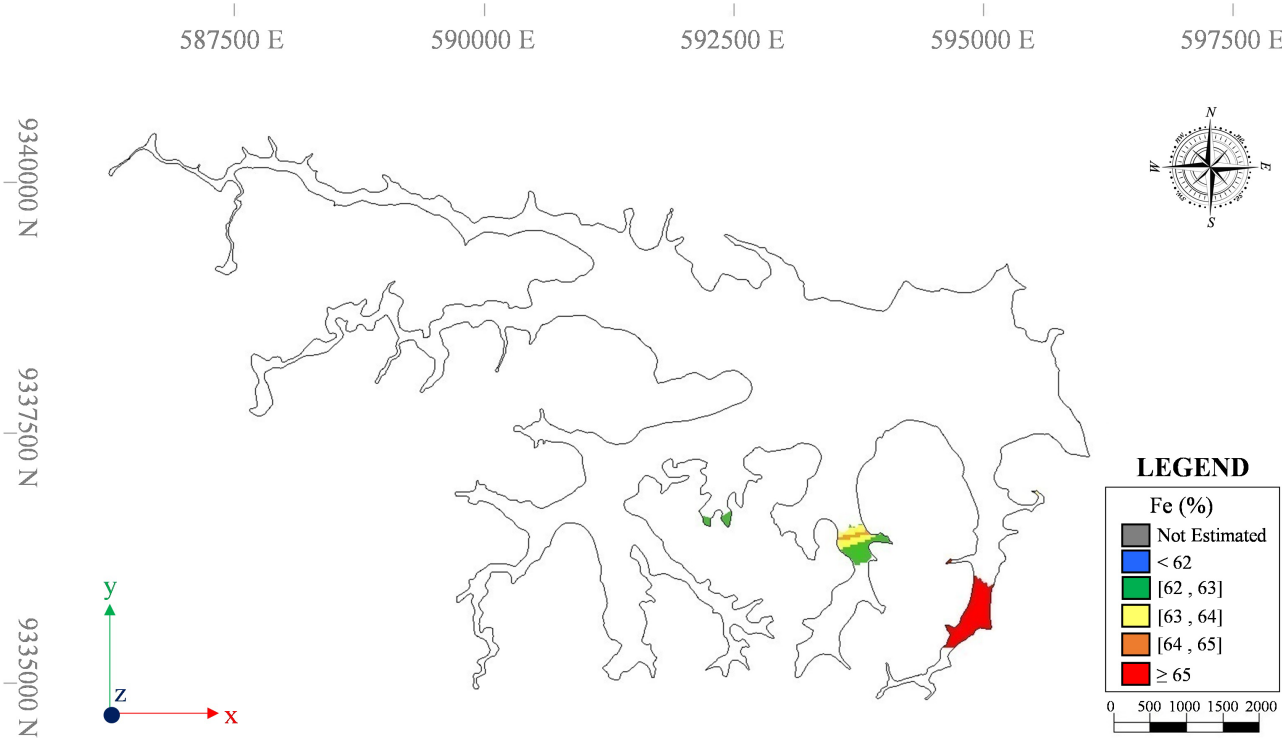

Figure 10. Plan view of the section at an elevation of 234.50 m of the block model estimated for Fe.

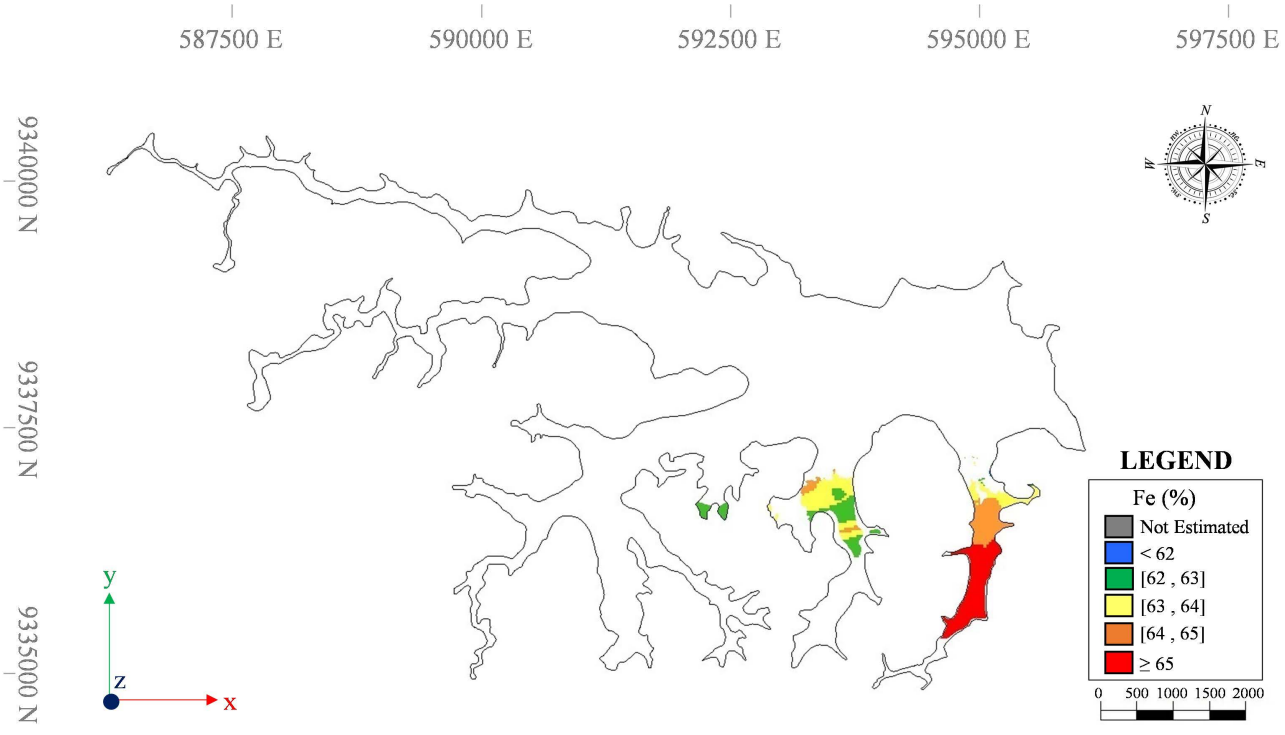

Figure 11. Plan view of the section at an elevation of 229.50 m of the estimated block model for Fe.

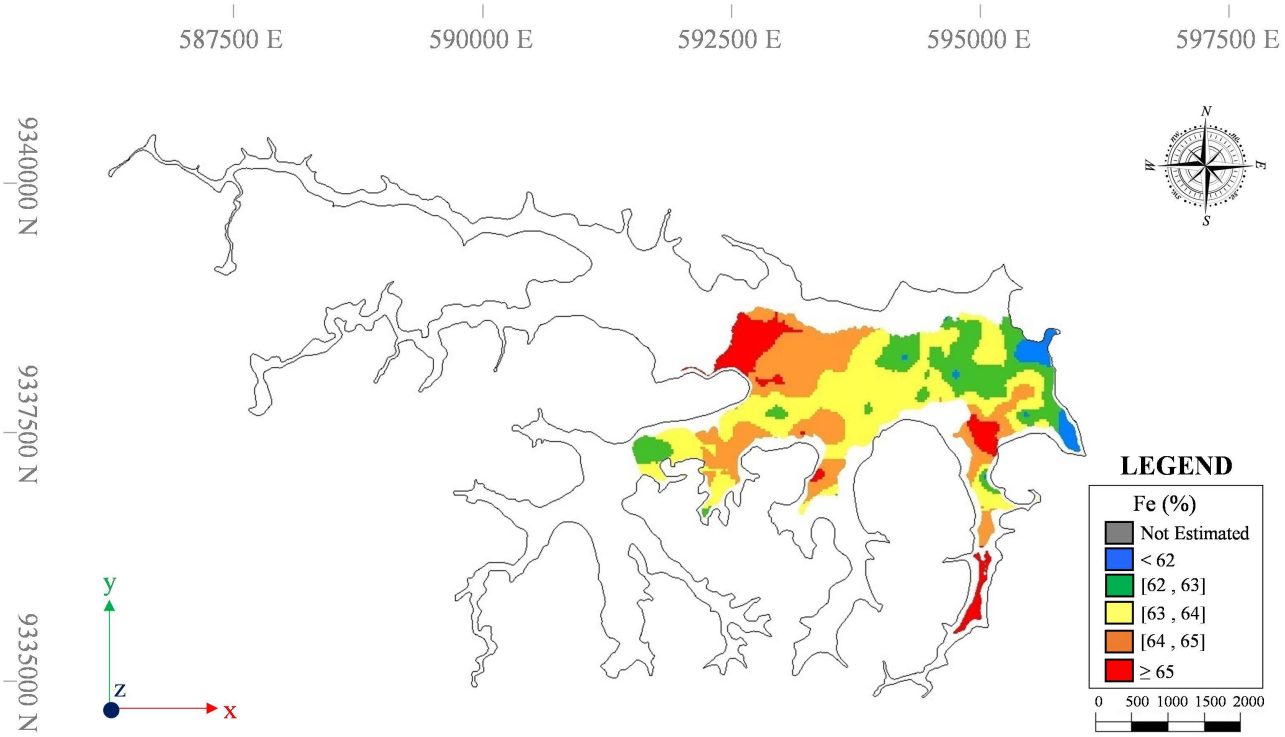

Figure 12. Plan view of the section at an elevation of 219.50 m of the estimated block model for Fe.

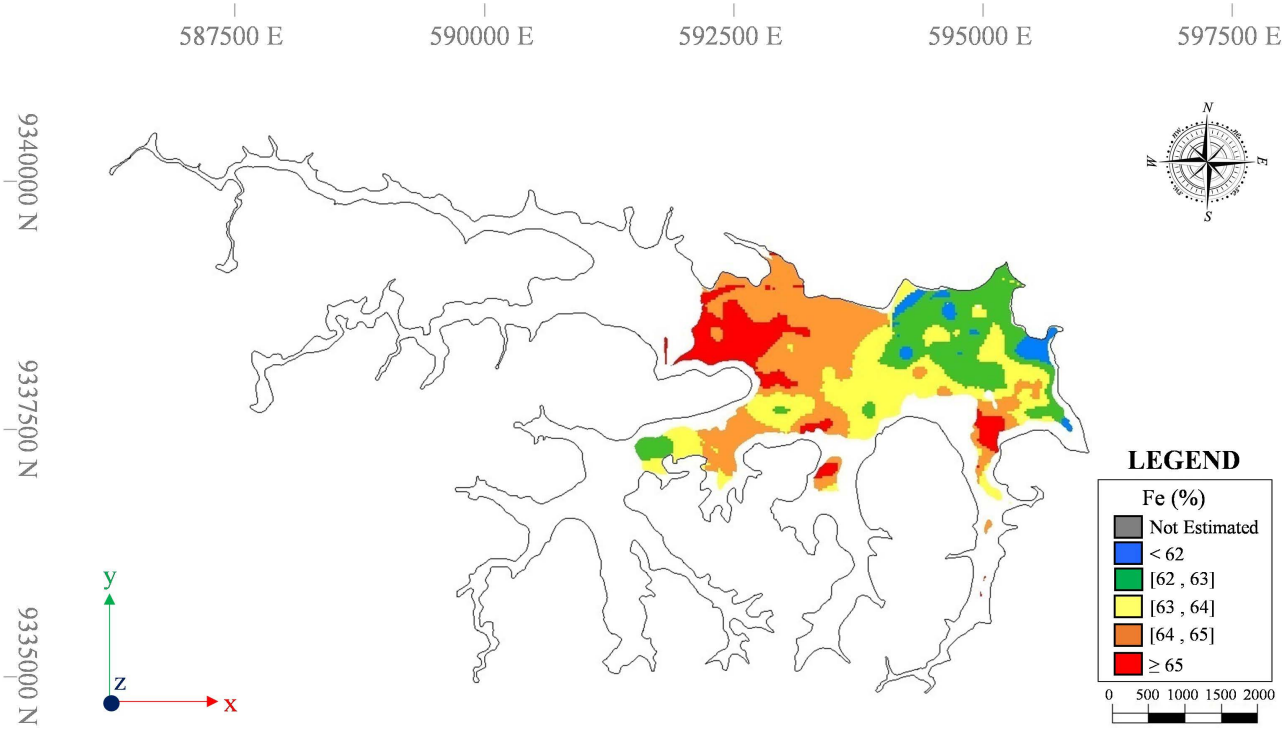

Figure 13. Plan view of the section at an elevation of 214.50 m of the estimated block model for Fe.

understanding of the spatial distribution of grades, improve the reliability of the estimates, and provide a solid basis for a future mineral resource classification, which is essential for economic feasibility analyses and planning of tailings repro-

cessing. Furthermore, densifying the drilling grid will enable a more accurate identification of high-grade zones, supporting safer and more sustainable decision-making in the management of the dam.

At an elevation of 219.50 m, corresponding to the water level of the dam, the highest Fe grades were concentrated in the far western region, exceeding 65%. Fe concentrations decreased toward the east, reaching 62% in the far eastern region. A similar pattern was observed at an elevation of 214.50 m, with areas showing Fe grades between 64% and 65% expanding in the western region, while Fe concentrations between 62% and 64% were more extensive in the eastern region.

4.4. Contributions to the Circular Economy

A more detailed characterization of the sediments deposited in tailings dams allows these materials to be reinterpreted from a new perspective — not merely as environmental liabilities to be monitored, but as potential sources of value that align with the concept of circular mining. A thorough analysis of their chemical composition, grain size distribution, and spatial variability enables the identification of fractions with significant metal contents, which can be reclassified as secondary resources. These materials, once considered waste, may be recovered through new beneficiation routes and emerging mineral reprocessing technologies.

A deeper understanding of the economic potential of tailings opens pathways for more integrated management and recovery strategies, making it possible to plan the controlled reprocessing of stored materials. This approach not only reduces the overall volume of discarded material but also mitigates environmental and structural risks, contributing to the remediation of degraded areas and the reduction of long-term liabilities. At the same time, it promotes synergies between operational efficiency, technological innovation, and social-environmental responsibility, which are essential elements in the transition toward more sustainable mining practices.

The reprocessing of tailings also supports the establishment of a closed-loop material cycle, where waste is reintegrated into the production chain as a valuable input. In doing so, it reduces the dependence on new mineral extraction and enhances the utilization of already exploited resources, in full alignment with the core principles of the circular economy—reduce, reuse, and recycle. This integrated perspective transforms an environmental challenge into a strategic opportunity, reinforcing the role of mining as a driver of innovation and sustainability in the responsible management of natural resources.

5. Conclusion

The present work aimed to develop knowledge about the tailings body of the dam of an iron mine in Brazil. By analyzing and validating the database of the drilling campaigns for the years 2001 and 2010, it was possible to ensure the use of the data for the target sequence of activities.

Three-dimensional geological modeling of the tailings body provided a detailed view of its geometry, while the descriptive statistics of the drillhole samples provided initial insights into the variability of the materials that were present. In terms of a spatial continuity analysis, the sampling grid proved to be sufficient for most of the chemical elements in the deposit, which contributed to variograms with good structures.

The estimation process implemented via kriging sought optimal estimation parameters. However, owing to the heterogeneity of the data and because certain regions had few samples, some chemical elements and particle size fractions could not be estimated. Even so, the validation of the estimate was quite satisfactory. When the estimated and ungrouped means were compared using the nearest-neighbor method, the difference between them was negligible. In the drift analysis, the swath plots produced in the three directions showed differences within the tolerable limits.

With the validated model, the total tonnage was 287.14 Mt, with an average Fe grade of 63.89%. For the tonnage calculation, the total model volume of 118.85 Mm^3 and an assumed average density of 2.50 t/m^3 were considered. However, for further study and a future formal resource classification, it is essential to conduct laboratory density tests on representative samples of the tailings. Obtaining measured density values will allow for a more accurate estimation of tonnage and grade, reducing uncertainties and enhancing the reliability of the geostatistical model. This will enable a more precise evaluation of the economic potential of the tailings dam and provide essential input for technical and economic feasibility studies related to the reprocessing and recovery of the deposited materials.

It can also be observed that the occurrence of Fe at depths below the water level was high (≥ 65%) in the far western region of the dam. These levels decreased toward the far eastern region, reaching their lowest levels (<62%). In the far southern regions of the dam and at higher elevations (above the water level), the concentration of Fe grades was higher (≥ 65%).

As a suggestion for a future perspective, and considering a resource classification with a lower degree of uncertainty, it is essential to carry out new drilling campaigns, especially in areas with lower sampling density. In this way, the spatial variability of grades can be characterized more representatively, reducing overestimation bias and increasing the reliability of the geostatistical model. Based on this improved understanding, it becomes possible to advance to subsequent technical stages, such as conducting metallurgical tests to evaluate the recoverability and performance of the material under different processing routes.

In parallel, conducting a preliminary economic analysis will allow for the estimation of costs, potential revenues, and financial viability indicators for tailings reprocessing. In this context, it is important to integrate into the study a preliminary mine planning assessment, considering different operational scenarios. This approach requires defining priority extraction zones based on grade, depth, and hydraulic accessibility criteria, as well as modeling optimized operational se-

quences to maximize economic return while minimizing environmental impacts.

Acknowledgements

The authors would like to thank Instituto Tecnológico Vale for the resources used to prepare this study.

Conflicts of Interest

The authors declared no potential conflicts of interest with respect to the research, authorship and/or publication of this paper.

References

Aquino, E. R., Navarro Torres, V. F., & Paniz, I. L. (2024). Tailings Dam Mining, Theoretical Considerations, and Circular Economy: A Review. *Journal of Geoscience and Environment Protection, 12,* 77-92. https://doi.org/10.4236/gep.2024.129005

Blannin, R., Frenzel, M., Tolosana-Delgado, R., Büttner, P., & Gutzmer, J. (2023). 3D Geostatistical Modelling of a Tailings Storage Facility: Resource Potential and Environmental Implications. *Ore Geology Reviews, 154,* Article 105337. https://doi.org/10.1016/j.oregeorev.2023.105337

Davis, J. C. (2002). *Statistics and Data Analysis in Geology* (3rd ed.). John Wiley & Sons.

Delfiner, P., & Delhomme, J. P. (1975). Optimum Interpolation by Kriging. In J. C. Davis, & M. J. McCullagh (Eds.), *Display and Analysis of Spatial Data* (pp. 96-114). John Wiley.

Deutsch, J. L., Szymanski, J., & Deutsch, C. V. (2014). Checks and Measures of Performance for Kriging Estimates. *Journal of the Southern African Institute of Mining and Metallurgy, 114,* 223-230.

Hunt, A. J., Anderson, C. W. N., Bruce, N., García, A. M., Graedel, T. E., Hodson, M. et al. (2014). Phytoextraction as a Tool for Green Chemistry. *Green Processing and Synthesis, 3,* 3-22. https://doi.org/10.1515/gps-2013-0103

Isaaks, E. H., & Srivastava, R. M. (1989). *An Introduction to Applied Geostatistics.* Oxford University Press.

Journel, A. G., & Huijbregts, C. J. (1978). *Mining Geostatistics.* Academic Press.

Kefeni, K. K., Msagati, T. A. M., & Mamba, B. B. (2017). Acid Mine Drainage: Prevention, Treatment Options, and Resource Recovery: A Review. *Journal of Cleaner Production, 151,* 475-493. https://doi.org/10.1016/j.jclepro.2017.03.082

Lottermoser, B. G. (2010). *Mine Wastes: Characterization, Treatment and Environmental Impacts* (3rd ed.). Springer.

Louwrens, E. L. (2016). *A Novel Geometallurgical Approach to Tailings Storage Facility Characterisation and Evaluation.* Master's Thesis, The University of Queensland.

New Century Resources (2017). *New Century Reports Outstanding Feasibility Results that Confirm a Highly Profitable, Large Scale Production & Low-Cost Operation for the Century Mine Restart.* https://announcements.asx.com.au/asxpdf/20171128/pdf/43pn3pvq59yjz5.pdf

Nikonow, W., Rammlmair, D., & Furche, M. (2019). A Multidisciplinary Approach Considering Geochemical Reorganization and Internal Structure of Tailings Impoundments for Metal Exploration. *Applied Geochemistry, 104,* 51-59. https://doi.org/10.1016/j.apgeochem.2019.03.014

Parviainen, A., Soto, F., & Caraballo, M. A. (2020). Revalorization of Haveri Au-Cu Mine

Tailings (SW Finland) for Potential Reprocessing. *Journal of Geochemical Exploration, 218,* Article 106614. https://doi.org/10.1016/j.gexplo.2020.106614

Poseidon Nickel (2020). *Gold Tailings Resource at Windarra Updated to JORC 2012.* https://www.marketindex.com.au/asx/pos/announcements/gold-tailings-resource-at-windarra-updated-to-jorc-2012-6A983245

Soto, F., Navarro, F., Díaz, G., Emery, X., Parviainen, A., & Egaña, A. (2022). Transitive Kriging for Modeling Tailings Deposits: A Case Study in Southwest Finland. *Journal of Cleaner Production, 374,* Article 133857. https://doi.org/10.1016/j.jclepro.2022.133857

Tripodi, E. E. M., Rueda, J. A. G., Céspedes, C. A., Vega, J. D., & Gómez, C. C. (2019). Characterization and Geostatistical Modelling of Contaminants and Added Value Metals from an Abandoned Cu-Au Tailing Dam in Taltal (Chile). *Journal of South American Earth Sciences, 93,* 183-202. https://doi.org/10.1016/j.jsames.2019.05.001

Vick, S. G. (1990). *Planning, Design, and Analysis of Tailings Dams.* BiTech Publishers Ltd.